

High Accuracy GMR Wheel Speed and Direction Sensor IC

FEATURES AND BENEFITS

- **GMR technology** integrates high sensitivity MR (magnetoresistive) sensor elements and high precision BiCMOS circuits on a single silicon integrated circuit, offering high accuracy, low magnetic field operation
- **Integrated capacitor** in a single overmolded miniature package provides greater EMC robustness
- **SolidSpeed Digital Architecture™** supports advanced algorithms, maintaining performance in the presence of extreme system-level disturbances, including vibration immunity capability over the full target pitch
- **Flexible orientation** for xMR or Hall replacement
- **ASIL B rating** based on integrated diagnostics and certified safety design process
- **Two-wire current source output** pulse-width protocol supporting speed, direction, and ASIL
- **EEPROM** offers device traceability throughout the production process



PACKAGE:



2-Pin SIP
(suffix UB)

Not to scale

DESCRIPTION

The A19350 is a giant magnetoresistance (GMR) integrated circuit (IC) that provides a user-friendly two-wire solution for applications where speed and direction information is required. The small integrated package includes an integrated capacitor and GMR IC in a single overmold design with an additional molded lead-stabilizing bar for robust shipping and ease of assembly.

The GMR-based IC is designed for use in conjunction with front-biased ring magnet encoders. State-of-the-art GMR technology with industry-leading signal processing algorithms accurately switch in response to low-level differential magnetic signals. The high sensitivity of GMR combined with differential sensing offers inherent rejection of interfering common-mode magnetic fields and valid speed and direction over larger air gaps, commonly required in wheel speed sensing applications.

Patented GMR technology allows the same orientation as Hall-effect for a drop-in solution in the application.

Integrated diagnostics are used to detect an IC failure which impacts the output protocol's accuracy, providing coverage compatible with ASIL B compliance. Built-in EEPROM scratch memory offers traceability of the device throughout the IC's production process.

The IC is offered in the UB package, which integrates the IC and a high-temperature ceramic capacitor in a single overmold SIP package for enhanced EMC performance. The 2-pin SIP package is lead (Pb) free, with tin leadframe plating.

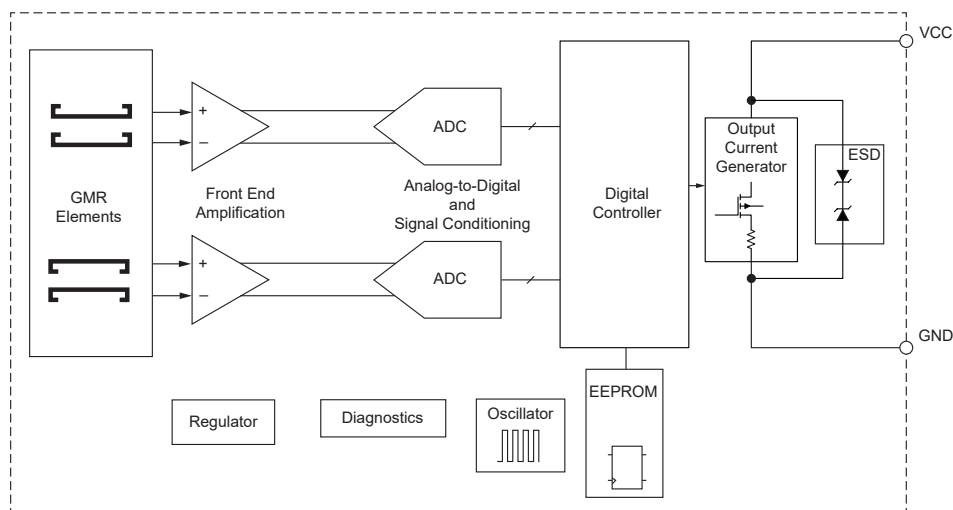


Figure 1: Functional Block Diagram

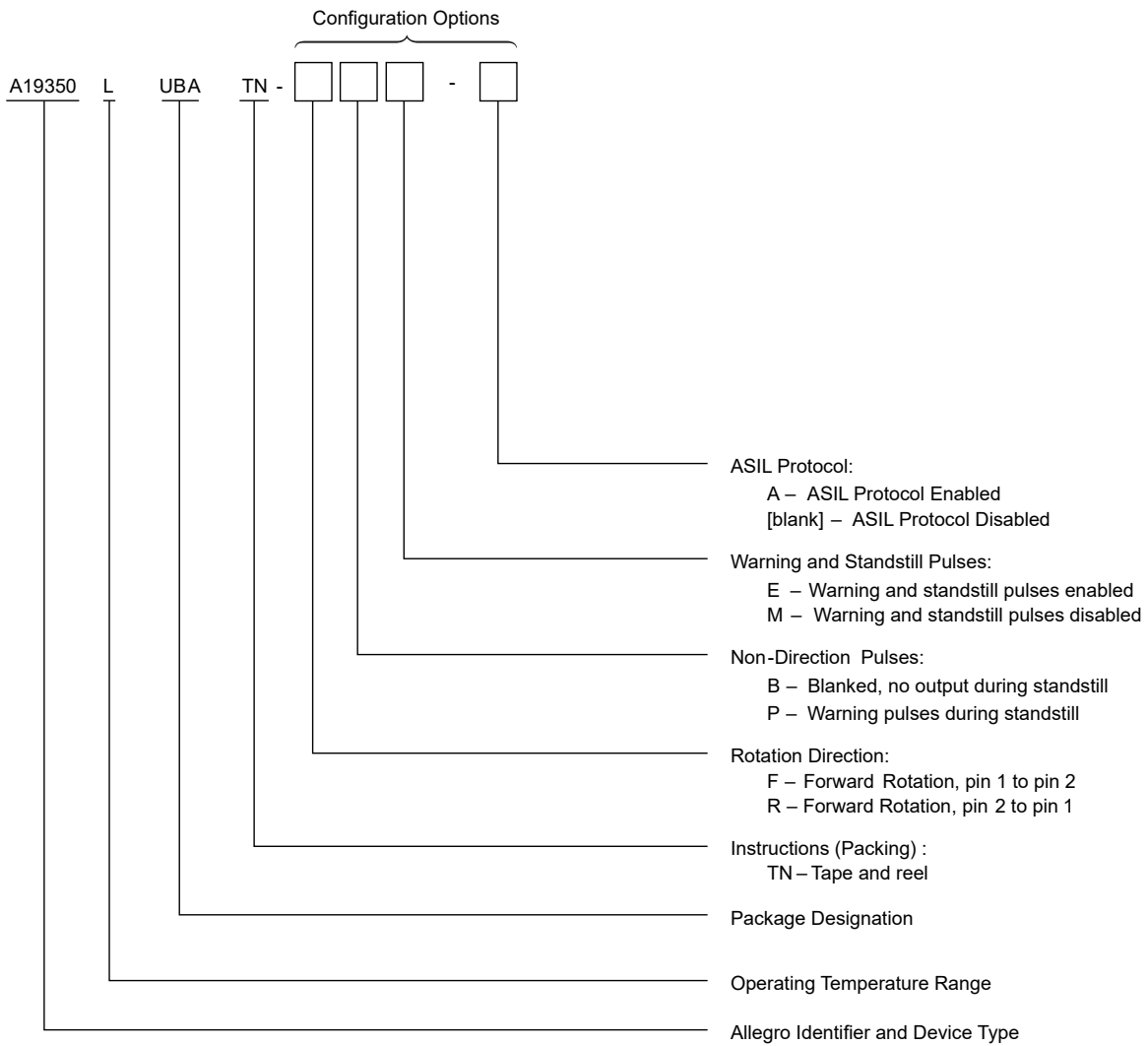
SELECTION GUIDE*

Part Number	Packing
A19350LUBATN-FBE	Tape and Reel, 4000 pieces per reel
A19350LUBATN-RBE	



* Not all combinations are available. Contact Allegro sales for availability and pricing of custom programming options.

Complete Part Number Format



SPECIFICATIONS

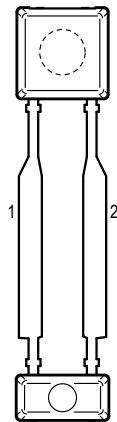
ABSOLUTE MAXIMUM RATINGS

Characteristic	Symbol	Notes	Rating	Unit
Supply Voltage	V_{CC}	Refer to Power Derating section; potential between pin 1 and pin 2	28	V
Reverse Supply Voltage	V_{RCC}		-18	V
Operating Ambient Temperature	T_A		-40 to 150	°C
Maximum Junction Temperature	$T_{J(max)}$		165	°C
Storage Temperature	T_{stg}		-65 to 170	°C
Applied Magnetic Flux Density	B	In any direction	500	G

INTERNAL DISCRETE CAPACITOR RATINGS

Characteristic	Symbol	Test Conditions	Value	Unit
Nominal Capacitance	C_{SUPPLY}	Connected between pin 1 and pin 2 (refer to Figure 2)	2.2	nF

PINOUT DIAGRAM AND TERMINAL LIST



Package UB, 2-Pin SIP Pinout Diagram

Terminal List Table

Pin Name	Pin Number	Function
VCC	1	Supply Voltage
GND	2	Ground

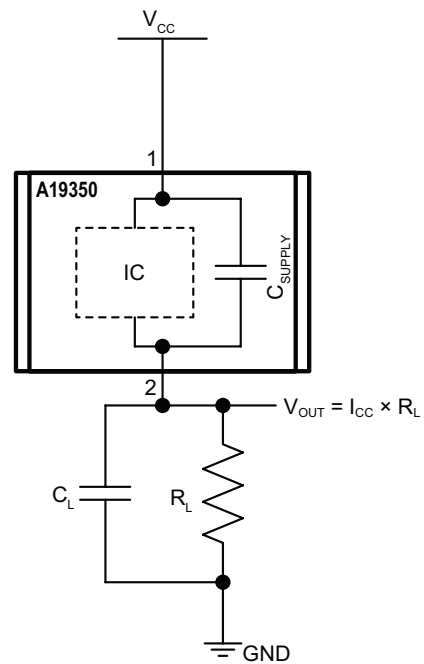


Figure 2: Application Circuit

OPERATING CHARACTERISTICS: Valid throughout full operating voltage and temperature ranges, unless otherwise specified

Characteristic	Symbol	Test Conditions	Min.	Typ. [1]	Max.	Unit
ELECTRICAL CHARACTERISTICS						
Supply Voltage [2]	V_{CC}	Potential between pin 1 and pin 2	4	–	24	V
Reverse Supply Current [3]	I_{RCC}	$V_{CC} = V_{RCC(MAX)}$	–10	–	–	mA
Supply Zener Clamp Voltage	$V_{Zsupply}$	$I_{CC} = I_{CC(MAX)} + 3 \text{ mA}$, $T_A = 25^\circ\text{C}$	28	–	–	V
Supply Current	$I_{CC(LOW)}$	Low-current state	5.9	7	8.4	mA
	$I_{CC(HIGH)}$	High-current state	12	14	16	mA
Supply Current Ratio [4]	$I_{CC(HIGH)}/I_{CC(LOW)}$	Measured as a ratio of high current to low current (isothermal)	1.9	–	–	–
ASIL Safety Current	I_{RESET}	Refer to Figure 11	1.5	3.5	3.9	mA
ASIL Safety Current Time	$t_{RESET(EP1)}$	Refer to Figure 11 (Error Protocol 1)	–	90	–	μs
	$t_{RESET(EP2)}$	Refer to Figure 11 (Error Protocol 2)	3	–	6	ms
Output Rise/Fall Time	t_r, t_f	Voltage measured at terminal 2 in Figure 2; $R_L = 100 \Omega$, $C_L = 10 \text{ pF}$, measured between 10% and 90% of signal	–	2	4	μs
POWER-ON CHARACTERISTICS						
Power-On State	POS	$V_{CC} > V_{CC(min)}$ as connected in Figure 1	$I_{CC(LOW)}$			mA
Power-On Time	t_{PO}	$V_{CC} > V_{CC(min)}$ as connected in Figure 1 [5]	–	–	1	ms
OUTPUT PULSE-WIDTH PROTOCOL [6]						
Pulse-Width Off Time	$t_{W(PRE)}$		38	45	52	μs
Forward Pulse Width	$t_{W(FWD)}$		76	90	104	μs
Reverse Pulse Width	$t_{W(REV)}$		153	180	207	μs
Warning Pulse Width	$t_{W(WARN)}$	-xxE variant	38	45	52	μs
Standstill Pulse Width	$t_{W(STILL)}$	-xxE variant	1232	1440	1656	μs
Standstill Period [7]	t_{STOP}	-xxE variant	590	737	848	ms

[1] Typical values are at $T_A = 25^\circ\text{C}$ and $V_{CC} = 12 \text{ V}$. Performance may vary for individual units, within the specified maximum and minimum limits.

[2] Maximum voltage must be adjusted for power dissipation and junction temperature; see representative Power Derating section.

[3] Negative current is defined as conventional current coming out of (sourced from) the specified device terminal.

[4] Supply current ratio is taken as a mean value of $I_{CC(HIGH)} / I_{CC(LOW)}$.

[5] Time between power-on to I_{CC} stabilizing. Output transients prior to t_{PO} should be ignored.

[6] Pulse width measured at threshold of $(I_{CC(HIGH)} + I_{CC(LOW)}) / 2$.

[7] At operating frequencies less than 2 Hz, -xxM variant must be used in order to output forward/reverse/warning direction pulses.

Continued on the next page...

OPERATING CHARACTERISTICS (continued): Valid throughout full operating voltage and temperature ranges, unless otherwise specified

Characteristic	Symbol	Test Conditions	Min.	Typ. [1]	Max.	Unit
INPUT CHARACTERISTICS AND PERFORMANCE						
Operating Frequency, Forward Rotation [8]	f_{FWD}		0	–	3.9	kHz
Operating Frequency, Reverse Rotation [8]	f_{REV}		0	–	2.4	kHz
Operating Frequency, Warning Pulses [8]	f_{WARN}		0	–	6.4	kHz
Operating Differential Magnetic Input [9]	$B_{DIFF(pk-pk)}$	Peak-to-peak of differential magnetic input (refer to Figure 6)	5	–	–	G
		Peak-to-peak allowable for repeatability (refer to Figure 6)	20	–	–	G
Operating Differential Magnetic Range [8]	B_{DIFF}	Refer to Figure 6	–50	–	50	G
Allowable Differential Sequential Signal Variation	$B_{SEQ(n+1)}/B_{SEQ(n)}$	Signal period-to-period variation (refer to Figure 3)	60	–	200	%
	$B_{SEQ(n+i)}/B_{SEQ(n)}$	Overall signal variation (e.g. run-out) (refer to Figure 3)	40	–	200	%
Operate Point	B_{OP}	% of peak-to-peak IC-processed signal	–	60	–	%
Release Point	B_{RP}	% of peak-to-peak IC-processed signal	–	40	–	%
Repeatability [10]	$Err_{\theta E}$	Constant air gap (greater than 20 G(pk-pk)), temperature, and target speed. Sinusoidal input signal. Greater than 1000 output edges captured.	–	–	0.3	%
Target Pitch	T_{PITCH}	Arc length of each pole-pair (at 0 mm air gap)	1.4	–	8	mm
Switch Point Separation	$B_{DIFF(SP-SEP)}$	Required amount of amplitude separated between channels at each B_{OP} and B_{RP} occurrence. (refer to Figure 5)	20	–	–	%pk-pk
THERMAL CHARACTERISTICS						
Magnetic Temperature Coefficient [11]	TC	Valid for full temperature range based on ferrite	–	0.2	–	%/°C
Package Thermal Resistance	$R_{\theta JA}$	Single-layer PCB with copper limited to solder pads	–	213	–	°C/W

[8] If a higher frequency operation is required, an option is available.

[9] Differential magnetic field is measured for the Channel A (E1-E3) and Channel B (E2-E4). Each channel's differential magnetic field is measured between two GMR elements spaced by 1.4 mm. Magnetic field is measured in the GMR element spacing orientation in the B_y direction (Refer to Figure 7). To maintain optimal performance, it is recommended that the $|B_x|$ field be less than 80 G.

[10] Repeatability (i.e. jitter) is tested to 6 sigma and is guaranteed by design and characterization only.

[11] Ring magnet decreases in magnetic strength with rising temperature, and the device compensates. Note that $B_{DIFF(pk-pk)}$ requirement is not influenced by this.

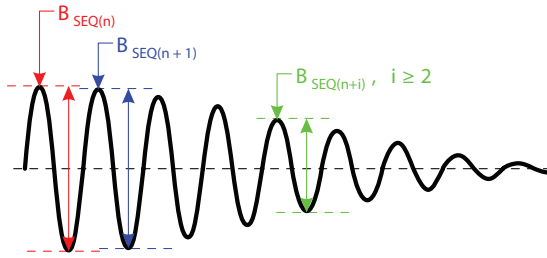
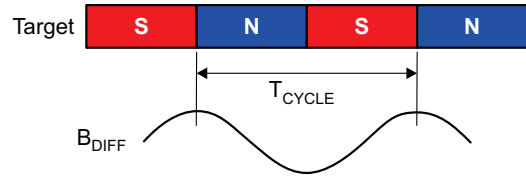


Figure 3: Differential Signal Variation



B_{DIFF} = Differential Input Signal; the differential magnetic flux sensed by the sensor
 T_{CYCLE} = Target Cycle; the amount of rotation that moves one north pole and one south pole across the sensor

Figure 4: Definition of T_{CYCLE}

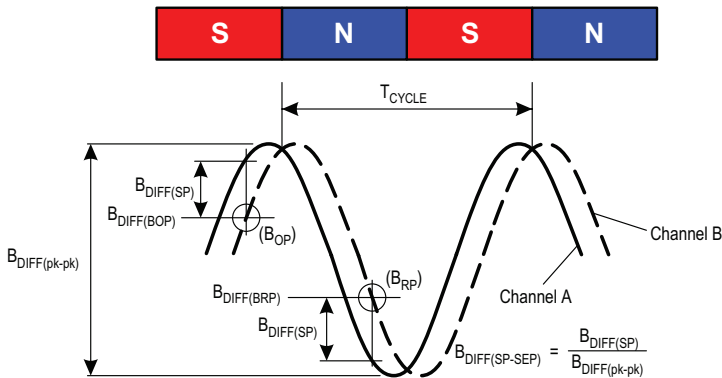


Figure 5: Definition of Switch Point Separation

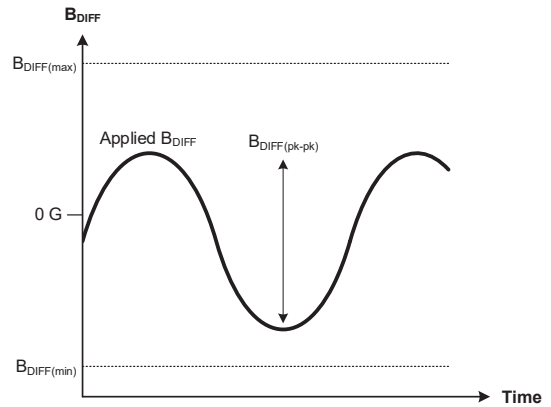


Figure 6: Input Signal Definition

FUNCTIONAL DESCRIPTION

The A19350 sensor IC contains a single-chip GMR circuit that uses spaced elements. These elements are used in differential pairs to provide electrical signals containing information regarding edge position and direction of rotation. The A19350 is intended for use with ring magnet targets as shown in Figure 8. The IC detects the peaks of the magnetic signals and sets dynamic thresholds based on these detected signals.

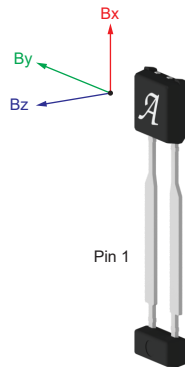


Figure 7: Package Orientation

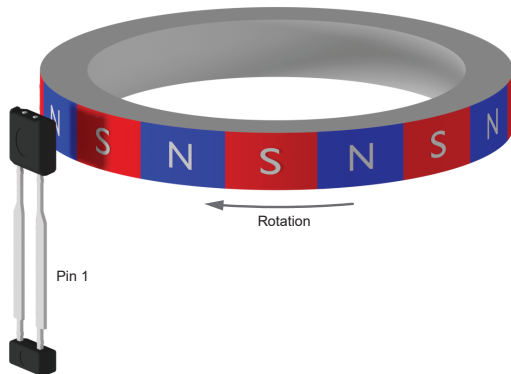


Figure 8: Parallel Orientation

Data Protocol Description

When a target passes in front of the device (opposite the branded face of the package case), the A19350 generates an output pulse for each magnetic pole-pair of the target. Speed information is provided by the output pulse rate, while direction of target rotation is provided by the duration of the output pulses. The sensor IC can sense target movement in both the forward and reverse directions.

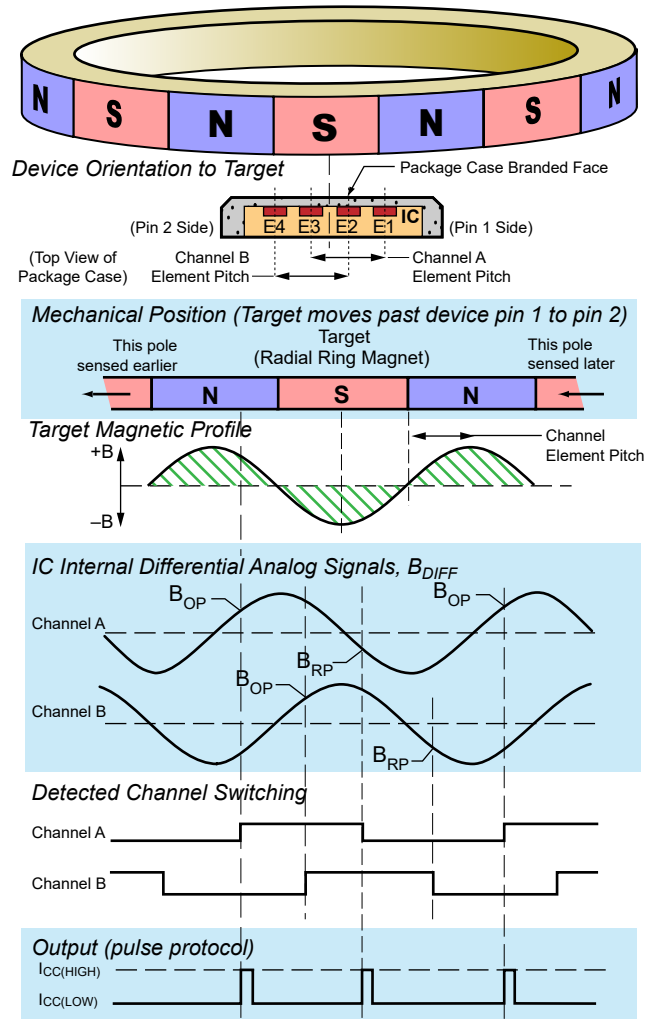


Figure 9: Basic Operation

Forward Rotation. For the -Fxx variant, when the target is rotating such that a target feature passes from pin 1 to pin 2, this is referred to as forward rotation. This direction of rotation is indicated on the output by a $t_{W(FWD)}$ pulse width. For the -Rxx variant, forward direction is indicated for target rotation from pin 2 to 1.

Reverse Rotation. For the -Fxx variant, when the target is rotating such that a target feature passes from pin 2 to pin 1, this is referred to as reverse rotation. This direction of rotation is indicated on the output by a $t_{W(REV)}$ pulse width. For the -Rxx variant, reverse direction is indicated for target rotation from pin 1 to 2.

Output edges are triggered by B_{DIFF} transitions through the switch points. On a crossing, the output pulse of $I_{CC(HIGH)}$ is present for $t_{w(FWD)}$ or $t_{w(REV)}$.

The IC is always capable of properly detecting input signals up to the defined operating frequency. At frequencies beyond the operational frequencies specifications (refer to Operational Frequency specifications noted on page 5), the $I_{CC(HIGH)}$ pulse duration will collide with subsequent pulses.

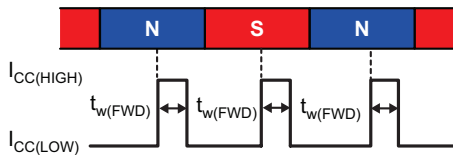


Figure 10: Output Timing Example

ASIL Safe State Output Protocol

The A19350 sensor IC contains diagnostic circuitry that will continuously monitor occurrences of failure defects within the IC. Refer to Figure 11 for the output protocol of the ASIL safe state after an internal defect has been detected. Error Protocol 1 will result from faults due to over frequency conditions from the input signal. Error Protocol 2 will result from hard failures detected within the A19350 such as a regulator and front end fault.

Note: If a fault exists continuously, the device will stay in permanent safe state. Refer to the A19350 Safety Manual for additional details on the ASIL Safe State Output Protocol.

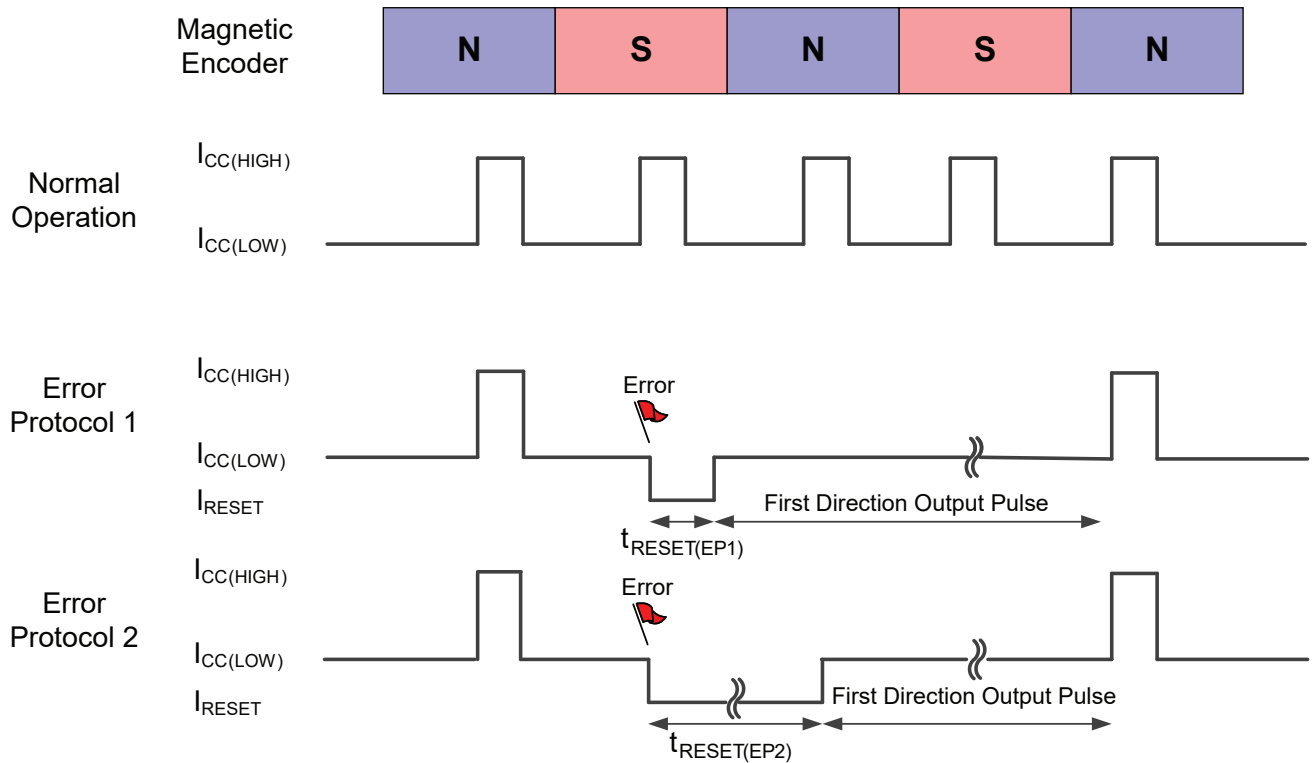


Figure 11: Output Protocol of the -xBx Variant (ASIL Safe State)

Calibration and Direction Validation

When power is applied to the A19350, the built-in algorithm performs an initialization routine. For a short period after power-on, the device calibrates itself and determines the direction of target rotation. For the -xPx variant, the output transmits non-direction pulses during calibration (Figure 12). For the -xBx variant, the output does not transmit any pulses during calibration.

Once the calibration routine is complete, the A19350 will transmit accurate speed and direction information.

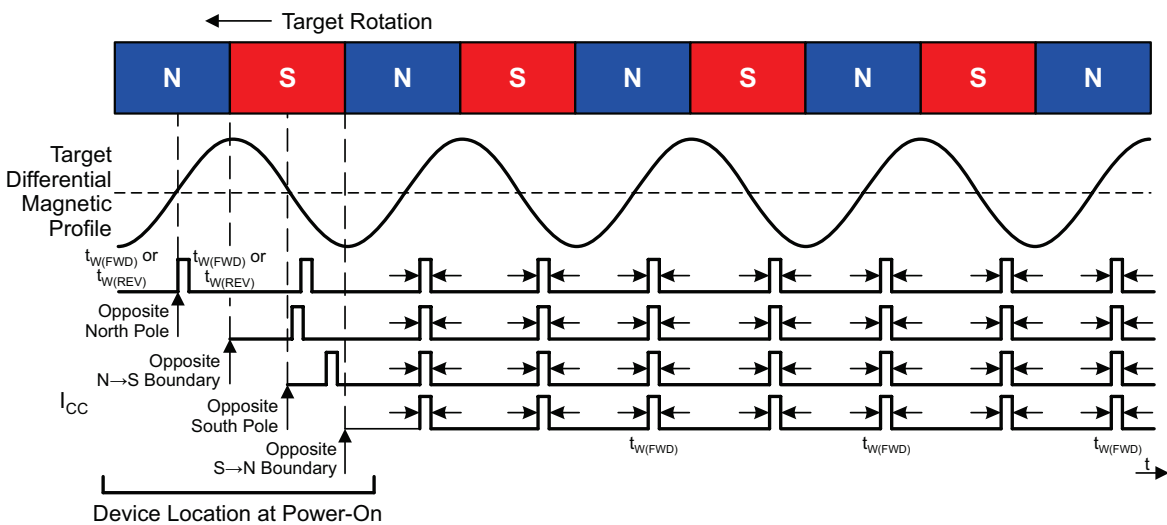


Figure 12: Calibration Behavior of the -xPx Variant

Direction Changes, Vibrations, and Anomalous Events

During normal operation, the A19350 will be exposed to changes in the direction of target rotation (Figure 13), vibrations of the target (Figure 14), and anomalous events such as sudden air gap changes. These events cause temporary uncertainty in the A19350’s internal direction detection algorithm.

The -xPx variant may transmit non-direction pulses during vibrations, while the -xBx variant will not transmit any pulses during vibrations.

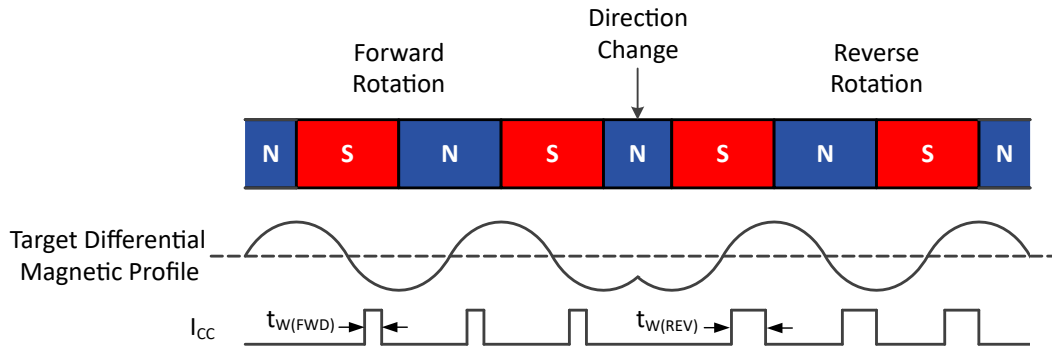


Figure 13: Direction Change Behavior

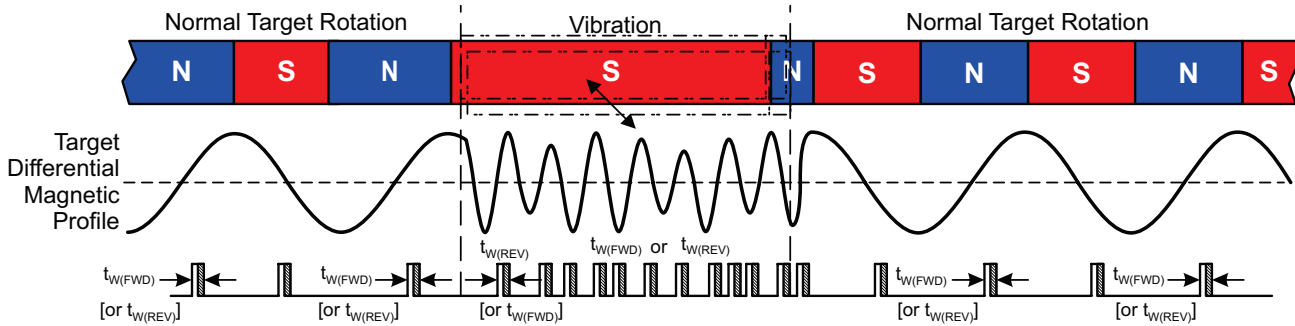


Figure 14: Vibration Behavior

POWER DERATING

The device must be operated below the maximum junction temperature of the device, $T_{J(max)}$. Under certain combinations of peak conditions, reliable operation may require derating supplied power or improving the heat dissipation properties of the application. This section presents a procedure for correlating factors affecting operating T_J . (Thermal data is also available on the Allegro MicroSystems website.)

The Package Thermal Resistance, $R_{\theta JA}$, is a figure of merit summarizing the ability of the application and the device to dissipate heat from the junction (die), through all paths to the ambient air. Its primary component is the Effective Thermal Conductivity, K , of the printed circuit board, including adjacent devices and traces. Radiation from the die through the device case, $R_{\theta JC}$, is a relatively small component of $R_{\theta JA}$. Ambient air temperature, T_A , and air motion are significant external factors, damped by overmolding.

The effect of varying power levels (Power Dissipation, P_D) can be estimated. The following formulas represent the fundamental relationships used to estimate T_J , at P_D .

$$P_D = V_{IN} \times I_{IN} \quad (1)$$

$$\Delta T = P_D \times R_{\theta JA} \quad (2)$$

$$T_J = T_A + \Delta T \quad (3)$$

For example, given common conditions such as:

$T_A = 25^\circ\text{C}$, $V_{CC} = 12\text{ V}$, $I_{CC} = 7.15\text{ mA}$, and $R_{\theta JA} = 213^\circ\text{C/W}$, then:

$$P_D = V_{CC} \times I_{CC} = 12\text{ V} \times 7.15\text{ mA} = 85.8\text{ mW}$$

$$\Delta T = P_D \times R_{\theta JA} = 85.8\text{ mW} \times 213^\circ\text{C/W} = 18.3^\circ\text{C}$$

$$T_J = T_A + \Delta T = 25^\circ\text{C} + 18.3^\circ\text{C} = 43.3^\circ\text{C}$$

A worst-case estimate, $P_{D(max)}$, represents the maximum allowable power level ($V_{CC(max)}$, $I_{CC(max)}$), without exceeding $T_{J(max)}$, at a selected $R_{\theta JA}$ and T_A .

Example: Reliability for V_{CC} at $T_A = 150^\circ\text{C}$.

Observe the worst-case ratings for the device, specifically:

$R_{\theta JA} = 213^\circ\text{C/W}$ (subject to change), $T_{J(max)} = 165^\circ\text{C}$, $V_{CC(max)} = 24\text{ V}$, and $I_{CC(AVG)} = 14.8\text{ mA}$. $I_{CC(AVG)}$ is computed using $I_{CC(HIGH)(max)}$ and $I_{CC(LOW)(max)}$, with a duty cycle of 84% computed from $t_{w(REV)(max)}$ on-time and $t_{w(PRE)(min)}$ off-time (pulse-width protocol).

Calculate the maximum allowable power level, $P_{D(max)}$. First, invert equation 3:

$$\Delta T_{max} = T_{J(max)} - T_A = 165^\circ\text{C} - 150^\circ\text{C} = 15^\circ\text{C}$$

This provides the allowable increase to T_J resulting from internal power dissipation. Then, invert equation 2:

$$P_{D(max)} = \Delta T_{max} \div R_{\theta JA} = 15^\circ\text{C} \div 213^\circ\text{C/W} = 70.4\text{ mW}$$

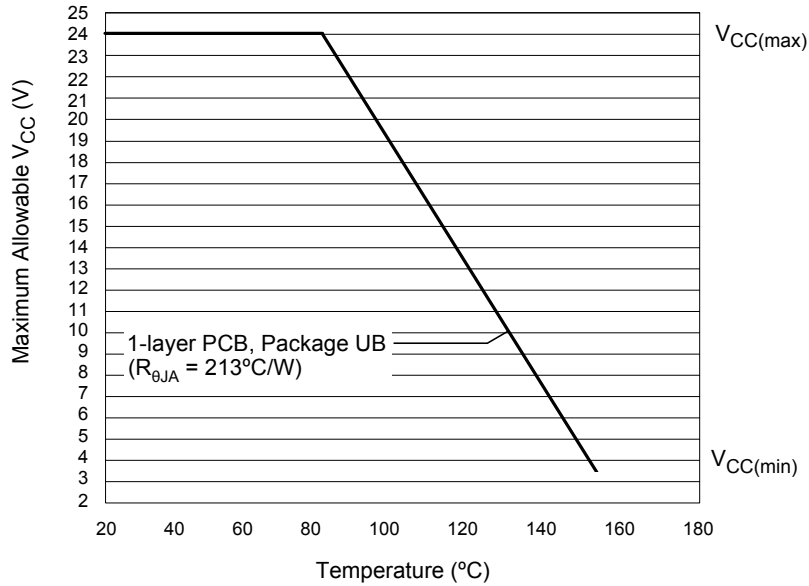
Finally, invert equation 1 with respect to voltage:

$$V_{CC(est)} = P_{D(max)} \div I_{CC(max)} = 70.4\text{ mW} \div 14.8\text{ mA} = 4.8\text{ V}$$

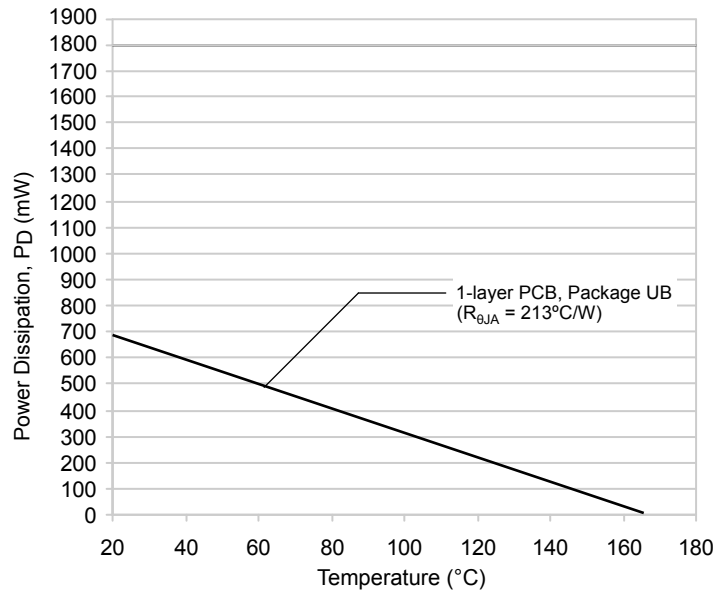
The result indicates that, at T_A , the application and device can dissipate adequate amounts of heat at voltages $\leq V_{CC(est)}$.

Compare $V_{CC(est)}$ to $V_{CC(max)}$. If $V_{CC(est)} \leq V_{CC(max)}$, then reliable operation between $V_{CC(est)}$ and $V_{CC(max)}$ requires enhanced $R_{\theta JA}$. If $V_{CC(est)} \geq V_{CC(max)}$, then operation between $V_{CC(est)}$ and $V_{CC(max)}$ is reliable under these conditions.

Power Derating Curve



Power Dissipation versus Ambient Temperature



PACKAGE OUTLINE DRAWING

For Reference Only – Not for Tooling Use

(Reference DWG-0000408, Rev. 3)
 Dimensions in millimeters – NOT TO SCALE
 Dimensions exclusive of mold flash, gate burs, and dambar protrusions
 Exact case and lead configuration at supplier discretion within limits shown

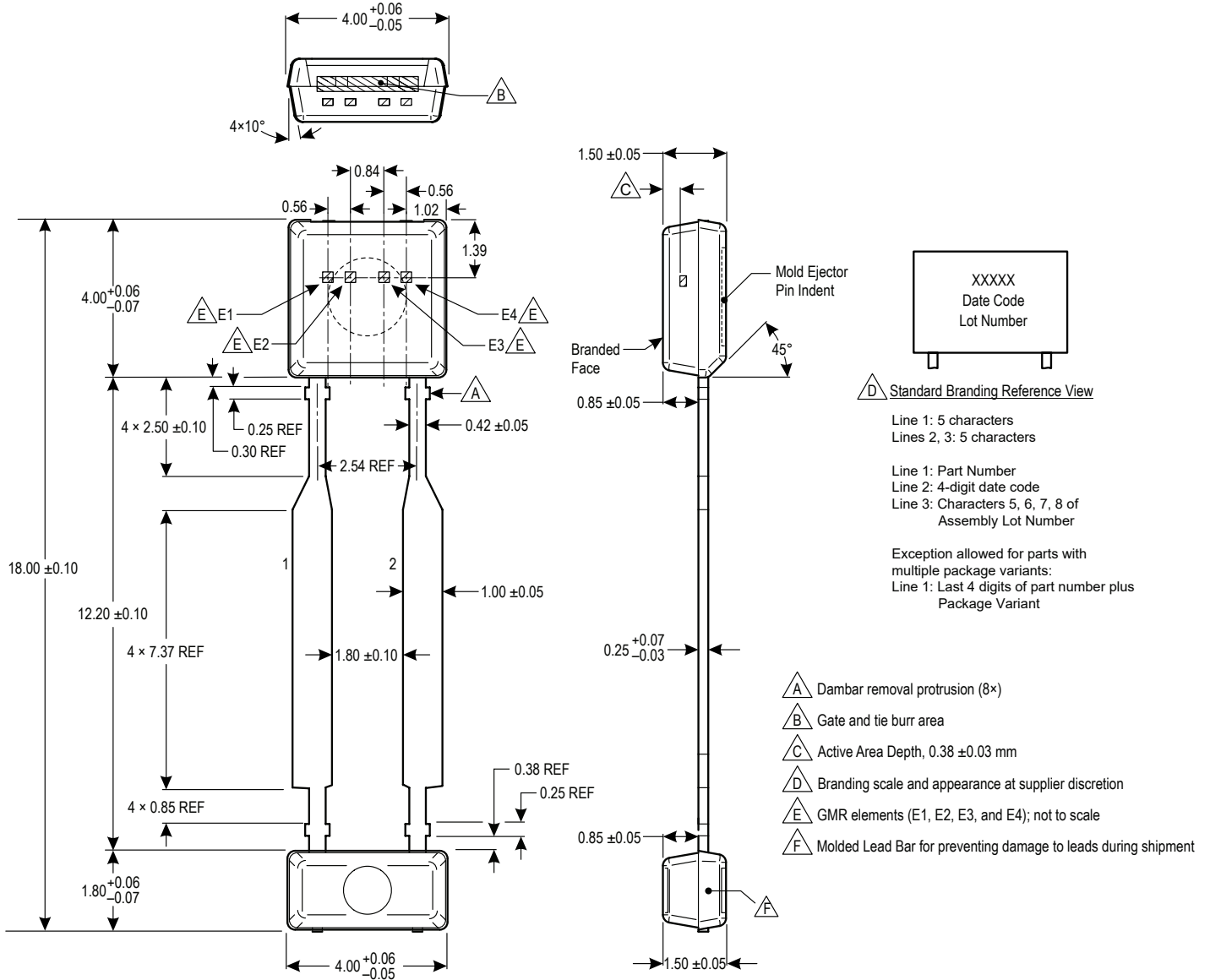


Figure 15: Package UB, 2-Pin SIP

Revision History

Number	Date	Description
-	November 16, 2018	Initial release

Copyright ©2018, Allegro MicroSystems, LLC

Allegro MicroSystems, LLC reserves the right to make, from time to time, such departures from the detail specifications as may be required to permit improvements in the performance, reliability, or manufacturability of its products. Before placing an order, the user is cautioned to verify that the information being relied upon is current.

Allegro's products are not to be used in any devices or systems, including but not limited to life support devices or systems, in which a failure of Allegro's product can reasonably be expected to cause bodily harm.

The information included herein is believed to be accurate and reliable. However, Allegro MicroSystems, LLC assumes no responsibility for its use; nor for any infringement of patents or other rights of third parties which may result from its use.

Copies of this document are considered uncontrolled documents.

For the latest version of this document, visit our website:

www.allegromicro.com

